


Hyperparametric frequency noise eater

Andrey B. Matsko*

OEWaves Inc., 465 North Halstead Street, Suite 140, Pasadena, California 91107, USA (Received 19 November 2018; revised manuscript received 21 January 2019; published 22 February 2019)

Nonlinear optical frequency conversion can result in redistribution of the noise of the coherent pump light among generated optical harmonics leading to improved quality of laser emission. The property is useful for making narrow line lasers suitable for various metrology applications on a chip. We show theoretically that the resonant hyperparametric scattering allows reducing optical frequency noise in one of the generated harmonics with respect to the coherent pump light. The reduction calls for significantly dissimilar quality factors of the resonator modes and appears at the cost of enhanced frequency sensitivity to power fluctuations of the pump light. The artificial suppression of the quality factor of one of the modes participating in the scattering does not lead to significant increase of the oscillation threshold and broadens the dynamic range of the phase matching of the process. The technique is promising for creation of chip-scale parametric frequency “noise eaters.”

DOI: [10.1103/PhysRevA.99.023843](https://doi.org/10.1103/PhysRevA.99.023843)**I. INTRODUCTION**

Optical sensors call for high spectral purity optical sources [1] to improve the measurement sensitivity [2–5]. The noise of the optical sources also defines performance of high data rate optical communications [6,7]. Solid state or fiber lasers stabilized to external bulk cavities are utilized to fulfill some of these requirements [8–10]. Further improvements are needed to create spectrally pure lasers that are small in size and insensitive to environmental perturbations to enable sensor arrays operating in harsh environments. This problem is partially solved by usage of optical monolithic microresonators for the semiconductor laser stabilization via self-injection locking [11–14]. The self-injection locking technique works well with single-mode semiconductor distributed feedback (DFB) lasers, calls for high stability and high transparency of the optical path between the laser chip and the resonator [15], and is prone to residual optical backscattering and ultimately requires optical isolators. It is desirable to create an optical system enabling reduction of the noise of any existing laser, independently of its nature. The requirement for usage of an optical isolator is also technologically stringent and undesirable for photonic integrated circuits. In this paper we show theoretically that a four-wave mixing hyperparametric frequency oscillator based on a monolithic microcavity solves the problem by cleaning the spectrum of a laser used for pumping this oscillator.

Active optical systems are able to reduce disorder associated with the incoherent pump and to produce coherent light. The simplest example of an active system that reduces noise of the optical pump is a laser itself. A laser transforms a practically incoherent pump into a coherent one. While the degree of the noise reduction is very large, frequently it is insufficient to achieve desirable spectral purity of the emitted coherent radiation. One of the reasons is that the laser noise

depends on the quality (Q) factor of the laser cavity, which is not very large, especially in semiconductor lasers.

It was known for years that stimulated Brillouin scattering (SBS) is an example of a nonlinear process in which generated light can have significantly lower phase noise compared with the phase noise of the pump light if the bandwidth of the optical modes is smaller than the bandwidth of the mechanical mode [16–20]. The extra optical noise brought to the system is transferred to the weakly coherent phonons also generated in the process. Recently the SBS-mediated optical noise-cleaning technique was expanded to generalized optomechanical structures. Optomechanical oscillations (OMOs) of these structures feature small internal noise described by a Schawlow-Townes-like model [21,22] which ultimately is much smaller than the noise of the optical pump [23–26]. The generated optical harmonic receives the pump noise so that the produced phonons become very coherent in the opposite case of the very high Q of the mechanical mode that can be achieved in an OMO. A phonon “laser” can be produced in this way [27].

SBS is a strongly nondegenerate parametric process in which a photon and a phonon are generated from a pump photon. A hyperparametric scattering in which two pump photons are converted to two degenerate harmonic photons is somewhat analogous to SBS and, hence, can be used for the reduction of the optical noise relatively to the noise of the pump light if the system has dissimilar decay rates for the modes participating in the process. We adopt a model of a resonant hyperparametric oscillator [28] to analyze the dependence of the frequency of harmonics of the hyperparametric oscillator on the frequency and power of the pump laser. Previously the analysis was performed for a nearly symmetric model of a hyperparametric oscillator with the focus at the beat note between the pump and generated light [29]. The ideal symmetry in the oscillation process results in the complete suppression of the influence of the pump parameters on the beat note frequency. The pump noise penetrates into the beat note if the symmetry is broken, and, hence, the

*andrey.matsko@oewaves.com

asymmetric case is undesirable if one intends to generate low noise radio frequency signals with the oscillator. In this paper we focus on the optical properties of the generated harmonics and find that the significantly asymmetric case is advantageous for improving the optical noise of a selected frequency harmonic produced in the system.

In the symmetric hyperparametric oscillator the frequency noise of the optical pump is imprinted on the generated optical harmonics in an identical way. Drift of the pump frequency results in identical drift of the harmonic frequencies. Due to this fact the noise of the beat note of the pump and harmonics does not depend on the pump frequency noise. We find that in the significantly asymmetric case, when one of the resonator modes containing the generated harmonic has a much higher Q factor, the frequency of light generated in this mode barely depends on the frequency of the pump light. The frequency of the light is locked to the frequency of the mode instead. Engineering the Q factor of the resonator modes allows reducing the optical frequency noise rather significantly. We show that the phase noise of the pump can be reduced by factor $4\gamma_+^2/\gamma_-^2$, where γ_\pm are the dissimilar, $\gamma_- \gg \gamma_+$, amplitude decay rates of the sideband modes. Since the hyperparametric oscillation can be strongly nondegenerate [30] one can easily filter out both the pump and the high noise frequency harmonic from the output light and use only the spectrally pure frequency harmonic.

In what follows we derive the basic equations describing resonant hyperparametric oscillator following Refs. [28,29] (Sec. II), we find their steady-state solution indicating that asymmetry of the attenuation rates results in increase of the phase-matching range of the oscillator as well as decrease of sensitivity of one of the generated harmonics to the pump frequency fluctuations (Sec. III), and we present an analysis of the quantum and classical noise in the system (Sec. IV). In Sec. V we discuss practical ways of achieving asymmetric decay rates in a nonlinear optical cavity and suggest an experimentally realizable system. Section VI concludes the paper.

II. BASIC EQUATIONS

We consider a hyperparametric oscillation in a nonlinear ring resonator. The model includes only three optical modes. The central mode is pumped optically. Two optical harmonics are generated in the outside modes. This is a four-wave mixing process in which two monochromatic optical pump photons transform into the two sideband photons. The oscillation is described by the Kerr Hamiltonian

$$V = -\hbar(g/2) : (a + b_+ + b_- + \text{H.c.})^4, \quad (1)$$

where “: . . . :” stands for normal ordering, a , b_+ , and b_- are the annihilation operators for the optically pumped and sideband modes, respectively, and g is the coupling constant defined as [28]

$$g = \omega_0 \frac{\hbar \omega c n_2}{\mathcal{V} n_0 n_0}, \quad (2)$$

where ω_0 is the carrier frequency, c is speed of light in the vacuum, \mathcal{V} is the mode volume (complete overlap of the

modes and a nearly degenerate hyperparametric process is assumed), and n_2 is cubic nonlinearity of the material.

Equations describing the amplitude of the electric field within the optical modes are derived from Eq. (1) in a rotation wave approximation:

$$\begin{aligned} \dot{a} = & -(i\omega_0 + \gamma_0)a + ig[a^\dagger a + 2b_+^\dagger b_+ + 2b_-^\dagger b_-]a \\ & + 2iga^\dagger b_+ b_- + F_0 + f_0, \end{aligned} \quad (3)$$

$$\begin{aligned} \dot{b}_+ = & -(i\omega_+ + \gamma_+)b_+ + ig[2a^\dagger a + b_+^\dagger b_+ + 2b_-^\dagger b_-]b_+ \\ & + igb_-^\dagger a^2 + f_+, \end{aligned} \quad (4)$$

$$\begin{aligned} \dot{b}_- = & -(i\omega_- + \gamma_-)b_- + ig[2a^\dagger a + 2b_+^\dagger b_+ + b_-^\dagger b_-]b_- \\ & + igb_+^\dagger a^2 + f_-, \end{aligned} \quad (5)$$

where ω_0 and ω_\pm are frequencies of the pumped and sideband modes, respectively, γ_0 and γ_\pm are the coupling-defined decay rates of the of the modes, respectively (we neglect the attenuation of the material), f_0 and f_\pm are the fluctuational forces that take into account quantum noise contributions (to be discussed later), $F_0 = [2\gamma_0 P_0 / (\hbar\omega_0)]^{1/2} \exp[-i(\omega t - \phi_{F_0})]$, P_0 is the power of the external pump, and ω is the carrier frequency of the external pump.

It is essential in this configuration that $\gamma_- \neq \gamma_0 \neq \gamma_+$. The case of equal as well as nearly equal decay rates was considered earlier. In this paper we show that the essential inequality of the rates allows achieving significant phase noise reduction in one of the generated harmonics of the system.

Equations (3)–(5) have to be supplied with expressions for the output field:

$$a_{out} = -(F_0 + f_0)\sqrt{\tau/2\gamma_0} + \sqrt{2\gamma_0\tau}b_\pm, \quad (6)$$

$$b_{out\pm} = -f_\pm\sqrt{\tau/2\gamma_\pm} + \sqrt{2\gamma_\pm\tau}b_\pm, \quad (7)$$

where τ is the round trip time of light in the cavity.

III. STEADY-STATE SOLUTION

We use notations of Refs. [28,29] and present the field operators as a sum of the expectation value (A and B_\pm) and quantum slow-varying amplitudes (\hat{a} and \hat{b}_\pm):

$$a = (A + \hat{a})e^{-i\omega t}, \quad b_\pm = (B_\pm + \hat{b}_\pm)e^{-i\tilde{\omega}_\pm t}, \quad (8)$$

where $\tilde{\omega}_+$ and $\tilde{\omega}_-$ are the carrier frequencies of generated optical harmonics obeying

$$2\omega = \tilde{\omega}_+ + \tilde{\omega}_-, \quad (9)$$

resulting from the energy and photon number conservation laws. In this section we find the oscillation threshold and values of $\tilde{\omega}_\pm$.

We drop the quantum terms and substitute (8) into (3)–(5) to derive a set of steady-state equations for A and B_\pm :

$$\Gamma_0 A = ig[|A|^2 + 2|B_+|^2 + 2|B_-|^2]A + 2igA^*B_+B_- + F_0, \quad (10)$$

$$\Gamma_+ B_+ = ig(2|A|^2 + 2|B_-|^2 + |B_+|^2)B_+ + igB_-^*A^2, \quad (11)$$

$$\Gamma_- B_- = ig(2|A|^2 + |B_-|^2 + 2|B_+|^2)B_- + igB_+^* A^2, \quad (12)$$

where

$$\begin{aligned} \Gamma_0 &= i(\omega_0 - \omega) + \gamma_0, \\ \Gamma_{\pm} &= i(\omega_{\pm} - \tilde{\omega}_{\pm}) + \gamma_{\pm} \end{aligned}$$

denote the complex parameters standing for detuning and attenuation as well as the external optical pumping.

To solve the equations it is convenient to introduce dimensionless parameters [28,29]:

$$\xi = \frac{g|A|^2}{\gamma_0}, \quad f = \left(\frac{g}{\gamma_0}\right)^{1/2} \frac{|F_0|}{\gamma_0}, \quad A = |A|e^{i\phi_0},$$

$$B_{\pm} = |B_{\pm}|e^{i\phi_{\pm}}, \quad \mathcal{B}_{\pm} = \frac{|B_{\pm}|}{|A|}, \quad \psi = \phi_{F_0} - \phi_0,$$

$$\phi = 2\phi_0 - \phi_+ - \phi_-, \quad \Delta_{\pm} = \frac{\omega_{\pm} - \tilde{\omega}_{\pm}}{\gamma_0}, \quad \Delta_0 = \frac{\omega_0 - \omega}{\gamma_0},$$

$$D = \frac{2\omega_0 - \omega_+ - \omega_-}{\gamma_0} \simeq \frac{\beta_2 c \omega_{FSR}^2}{\gamma_0 n_0},$$

where $\omega_{FSR} \equiv (\omega_+ - \omega_-)/2$ is the free spectral range of the resonator in the vicinity of the pumped mode, β_2 is the group velocity dispersion (GVD) parameter for the resonator mode family (the parameter takes into account both geometrical and material contributions).

It is easy now to transform the set of three equations (10)–(12) to the set of six algebraic equations using this parametrization:

$$\sqrt{\xi}(1 - 2\xi\mathcal{B}_+\mathcal{B}_- \sin \phi) = f \cos \psi, \quad (13)$$

$$\begin{aligned} \sqrt{\xi}\{\Delta_0 - \xi[1 + 2(\mathcal{B}_+^2 + \mathcal{B}_-^2 + \mathcal{B}_+\mathcal{B}_- \cos \phi)]\} \\ = f \sin \psi, \end{aligned} \quad (14)$$

$$\gamma_+\mathcal{B}_+ + \gamma_0\xi\mathcal{B}_- \sin \phi = 0, \quad (15)$$

$$[\Delta_+ - \xi(2 + \mathcal{B}_+^2 + 2\mathcal{B}_-^2)]\mathcal{B}_+ - \xi\mathcal{B}_- \cos \phi = 0, \quad (16)$$

$$\gamma_-\mathcal{B}_- + \gamma_0\xi\mathcal{B}_+ \sin \phi = 0, \quad (17)$$

$$[\Delta_- - \xi(2 + 2\mathcal{B}_+^2 + \mathcal{B}_-^2)]\mathcal{B}_- - \xi\mathcal{B}_+ \cos \phi = 0, \quad (18)$$

$$\Delta_+ + \Delta_- = 2\Delta_0 - D \quad (\tilde{\omega}_+ + \tilde{\omega}_- = 2\omega). \quad (19)$$

The entire set of parameters describing the system (ξ , ϕ , Δ_+ , Δ_- as well as the ratio between \mathcal{B}_+ and \mathcal{B}_-) is derived from Eqs. (15)–(19):

$$\xi^2 = \frac{\gamma_+\gamma_-}{\gamma_0^2} + \frac{\gamma_+\gamma_-}{(\gamma_+ + \gamma_-)^2} \quad (20)$$

$$\begin{aligned} \{2\Delta_0 - D - \xi[4 + 3(\mathcal{B}_+^2 + \mathcal{B}_-^2)]\}^2, \\ \sin \phi = -\frac{\sqrt{\gamma_+\gamma_-}}{\gamma_0\xi}, \end{aligned} \quad (21)$$

$$\cos \phi = \frac{\{2\Delta_0 - D - \xi[4 + 3(\mathcal{B}_+^2 + \mathcal{B}_-^2)]\}\sqrt{\gamma_+\gamma_-}}{(\gamma_+ + \gamma_-)\xi}, \quad (22)$$

$$\begin{aligned} \Delta_+ &= (2\Delta_0 - D)\frac{\gamma_+}{\gamma_- + \gamma_+} \\ &+ \xi(2 + \mathcal{B}_+^2 + \mathcal{B}_-^2)\frac{\gamma_- - \gamma_+}{\gamma_- + \gamma_+}, \end{aligned} \quad (23)$$

$$\begin{aligned} \Delta_- &= (2\Delta_0 - D)\frac{\gamma_-}{\gamma_- + \gamma_+} \\ &- \xi(2 + \mathcal{B}_+^2 + \mathcal{B}_-^2)\frac{\gamma_- - \gamma_+}{\gamma_- + \gamma_+}, \end{aligned} \quad (24)$$

$$\frac{\mathcal{B}_+}{\mathcal{B}_-} = \sqrt{\frac{\gamma_-}{\gamma_+}}. \quad (25)$$

Using Eqs. (7) and (25) we find that the amplitude of the fields leaving the cavity is always the same:

$$\frac{|B_{out+}|}{|B_{out-}|} = \sqrt{\frac{\gamma_+ \mathcal{B}_+}{\gamma_- \mathcal{B}_-}} = 1. \quad (26)$$

We derive equations for phase ψ from Eq. (13) and Eq. (14). To simplify the equations we note that $\gamma_-\mathcal{B}_-^2 = \gamma_+\mathcal{B}_+^2$ and keep only terms dependent on \mathcal{B}_- :

$$\cos \psi = \frac{\sqrt{\xi}}{f} \left[1 + 2\frac{\gamma_-}{\gamma_0}\mathcal{B}_-^2 \right], \quad (27)$$

$$\begin{aligned} \sin \psi &= \frac{\sqrt{\xi}}{f} \left\{ \Delta_0 - \xi - 2\xi\mathcal{B}_-^2 \left[\frac{(\gamma_- - \gamma_+)^2}{\gamma_+(\gamma_+ + \gamma_-)} \right. \right. \\ &\left. \left. + \frac{\gamma_-(2\Delta_0 - D)}{\xi(\gamma_+ + \gamma_-)} - 3\frac{\gamma_-}{\gamma_+}\mathcal{B}_-^2 \right] \right\}. \end{aligned} \quad (28)$$

The equation for the intracavity field amplitude (\mathcal{B}_-) can be found from these equations ($\cos^2 \psi + \sin^2 \psi = 1$) as well as from Eq. (20):

$$\begin{aligned} \left[1 + 2\frac{\gamma_-}{\gamma_0}\mathcal{B}_-^2 \right]^2 + \left\{ \Delta_0 - \xi - 2\xi\mathcal{B}_-^2 \left[\frac{(\gamma_- - \gamma_+)^2}{\gamma_+(\gamma_+ + \gamma_-)} \right. \right. \\ \left. \left. + \frac{\gamma_-(2\Delta_0 - D)}{\xi(\gamma_+ + \gamma_-)} - 3\frac{\gamma_-}{\gamma_+}\mathcal{B}_-^2 \right] \right\}^2 = \frac{f^2}{\xi}. \end{aligned} \quad (29)$$

Equations (20) and (29) show that the threshold value of the normalized pump power f^2 depends on the bandwidth of the modes accommodating the generated sidebands. The oscillation conditions can be further simplified for the soft excitation regime characterized with $\mathcal{B}_{\pm}^2 \rightarrow 0$ in the vicinity of the threshold of the oscillation:

$$\xi(1 + [\Delta_0 - \xi]^2) = f^2, \quad (30)$$

$$\xi^2 = \frac{\gamma_+\gamma_-}{\gamma_0^2} + \frac{\gamma_+\gamma_-}{(\gamma_+ + \gamma_-)^2} [2\Delta_0 - D - 4\xi]^2. \quad (31)$$

A. Threshold and stability of the oscillations

Equations (30) and (31) do not take into account dynamic stability of the oscillations as well as stability of the oscillations with respect to the initial conditions, and, hence, the solution of the equations cannot always be realized experimentally. In this section we evaluate the threshold conditions by solving set (3)–(5) numerically at various values of dispersion parameter D and compare the result with the analytical

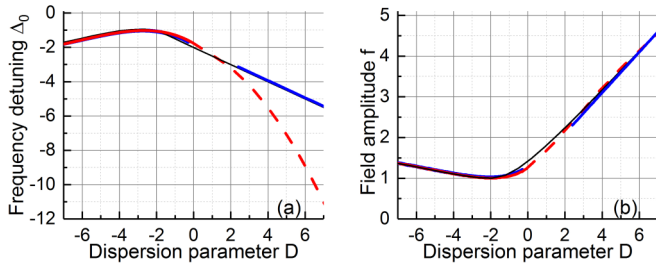


FIG. 1. Illustration of the oscillation threshold conditions for the case of three identical modes ($\gamma_{\pm} = \gamma_0$). (a) The detuning, Δ_0 , and (b) the pump amplitude, f , at the threshold. The red solid line stands for the hard excitation, the blue solid line stands for the soft excitation, and the red dashed line stands for the hard excitation unstable with respect to the initial conditions. The soft and hard excitation thresholds coincide for the anomalous GVD ($D < 0$). There is a limited stable oscillation regime for the case of normal GVD [31]. The thin solid line stands for solution of Eqs. (30) and (31).

model [(30), (31)]. To identify the threshold we varied free parameters f and Δ_0 and inferred the generated sideband power. The threshold of the oscillation was identified as the minimal value of f when the sideband power is different from zero.

During the simulations we used either nearly zero initial conditions for the soft excitation regime or random nonzero initial conditions for the hard excitation regime. More specifically, in the case of soft excitation we solved the set of ordinary differential equations starting from an optical power of a half of a photon in each mode. For the hard excitation regime we assumed that the initial number of photons in the modes is arbitrary, but not exceeding the resonant steady-state photon number corresponding to the selected pump value. The phase of the initial mode excitation was random in both cases. To verify the dynamical stability of the system we introduce a weak noise to the pump and ran the simulation over hundreds of ring-down times of the cavity, which leads to collapse of the dynamically unstable realizations. The simulations were performed for the case of identical modes as well as for the cases when the bandwidth of one of the sideband modes exceeds the bandwidth of the other two modes by 3 and 10 times. The evaluated threshold conditions are illustrated by Figs. 1, 2, and 4.

For the completely symmetric case, when all the modes have the same Q factor, the analytical model gives identical result with the numerical simulations for anomalous GVD (approximately $D < -0.3$) and large normal GVD (approximately $D > 2.3$), as shown in Fig. 1. The system becomes unstable with respect to initial conditions at $2.3 > D > -0.3$. Interestingly, while the threshold pump power followed the analytical result for the hard excitation, the frequency detuning value deviated from the analytical one. The larger detuning was selected by the system to compensate for the large generated harmonic values, since the oscillations with small harmonic amplitudes was not realized in the case of hard excitation.

As was found earlier [31], soft excitation is possible for $D > 4/\sqrt{3}$ and $-(D/2 + \sqrt{D^2 + 16})/2 > \Delta_0 >$

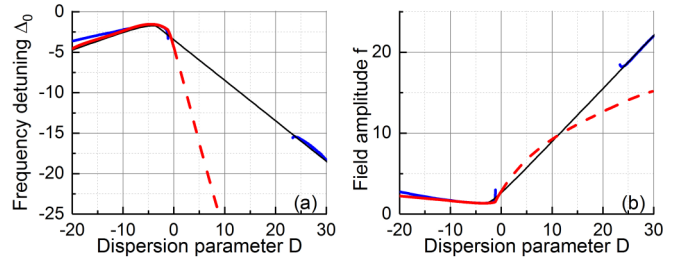


FIG. 2. Illustration of the oscillation threshold conditions for the case of $\gamma_+ = \gamma_0$ and $\gamma_- = 3\gamma_0$. (a) The detuning, Δ_0 , and (b) the pump amplitude, f , at the threshold. The red solid line stands for the hard excitation, the blue solid line stands for the soft excitation, and the red dashed line stands for the hard excitation unstable with respect to the initial conditions. The soft and hard excitation thresholds nearly coincide for the anomalous GVD ($D < 0$). An island of soft excitation occurs at normal GVD ($D > 0$), similarly to the symmetric case. The hard excitation has a lower threshold for normal GVD, but the oscillations are unstable with respect to the initial conditions. The thin solid line stands for solution of Eqs. (30) and (31).

$-(\sqrt{3} + D/2)$. The soft excitation is also supported for a limited interval of values of the pump, f . The soft and hard excitations have nearly identical power threshold values.

Increase of the asymmetry of the system attenuation resulted in a modification of the distribution of the stability windows for the oscillator. The soft excitation regime was stable in the region of the anomalous GVD, similarly to the case of symmetric loading of the modes. The oscillation was also stabilized at some normal GVD values with the stability region shifted to the higher pump power, as shown by the blue solid line in Fig. 2. The minimal achievable threshold value with respect to the pump power increased only slightly, in agreement with expression $f_{min}^2 \sim (\gamma_+ \gamma_-)^{1/2} / \gamma_0$. The parameters of the stability regions nearly coincided with the analytical model in the case of the soft excitation.

In the case of the hard excitation regime the simulation result nearly coincides with the analytical model for anomalous GVD. A lower power threshold than predicted by the analytical model can be realized for normal GVD values, as indicated by the dashed red line in Fig. 2. These solutions, though, are unstable with respect to the initial conditions.

It is instructive to illustrate the oscillation stability island observed at the conditions of normal GVD. To do it we create a density plot showing normalized power of the generated sidebands as a function of the pump power as well as pump frequency detuning (Fig. 3). In this plot one can see that there is a finite region of parameters where the stable oscillation is observed. This regime can be achieved for both soft and hard excitation conditions. The hard excitation is also realizable at larger detunings and at smaller pump powers. This regime is unstable with respect to the initial conditions. We select the initial conditions randomly, and, hence, the instability is visible because of the sparse distributed colored dots at the left-hand side of Fig. 3(a).

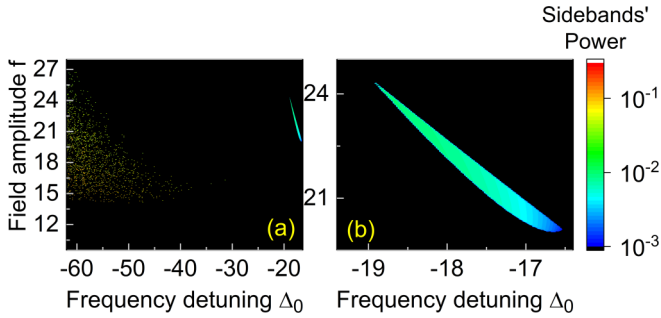


FIG. 3. Color density map plot illustrating dependence of the generated sidebands power on the detuning Δ_0 and pump amplitude f for the case of $\gamma_+ = \gamma_0$ and $\gamma_- = 3\gamma_0$ as well as $D = 27$ (normal GVD). (a) Hard and soft excitation regimes. The lowest point of the plot shows the position of the oscillation threshold illustrated by Fig. 2. The hard excitation region of parameters is observed when Δ_0 is large and negative. The value of f is smallest in this case, but the oscillations are unstable with respect to the initial conditions. The soft excitation is observed at smaller negative detunings and larger f values. (b) Inset showing the localized soft excitation region.

In the present study we are interested in the case of significantly dissimilar Q factors of the modes supporting generation of the frequency sidebands, since the asymmetry of the bandwidths of the modes leads to the generation of the spectrally pure light. Further increase of the asymmetry degree of the system results in stabilization of the oscillation at the normal GVD regime; see Fig. 4. It is also stable in the anomalous GVD region. The increase of the threshold power is moderate. The stable normal GVD regime, though, has a higher threshold if compared with the value found from the analytical expression. The frequency detuning value corresponding to this normal GVD regime is nearly identical with the analytical prediction. The power of the generated harmonics is illustrated by Fig. 5 (anomalous GVD) and Fig. 6 (normal GVD). The points of the distributions showing the smallest value of the pump found at the optimal detuning are used to draw Fig. 4. The parametric process can be very

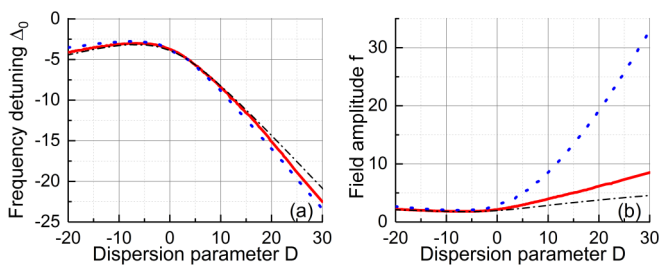


FIG. 4. Illustration of the oscillation threshold conditions for the case of $\gamma_+ = \gamma_0$ and $\gamma_- = 10\gamma_0$. (a) The detuning, Δ_0 , and (b) the pump amplitude, f , at the threshold. The red solid line stands for the hard excitation, and the blue dotted line stands for the soft excitation. The optimal detuning values for the soft and hard excitation threshold nearly coincide at any GVD within the studied parameter range. Hard excitation shows a lower threshold value; however, it is still higher than the threshold predicted by the solution of Eqs. (30) and (31), shown by the dash-dot black line. All the shown solutions are stable.

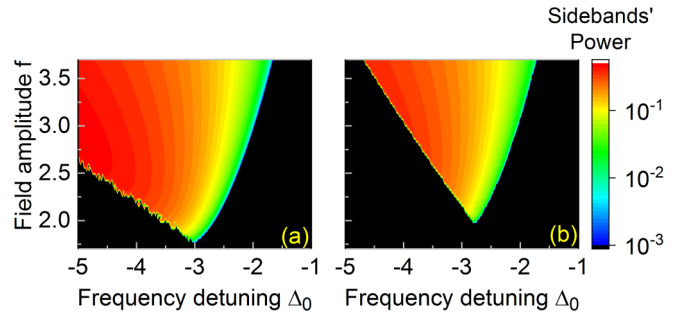


FIG. 5. Color density map plot illustrating dependence of the generated sidebands power on the detuning Δ_0 and pump amplitude f for the case of $\gamma_+ = \gamma_0$ and $\gamma_- = 10\gamma_0$ as well as $D = -6$. Panels (a) and (b) illustrate hard and soft excitation regimes, respectively. The lowest point of the plot shows the position of the oscillation threshold illustrated by Fig. 4.

efficient, so at least half of the pump power is transferred to the power of the generated harmonics.

IV. FLUCTUATIONS

It was shown previously that for the case of symmetric loading of the side modes, $\gamma_- = \gamma_+$, the relative frequency of the beat note of the pump and sideband harmonics does not depend on both the phase and the power of the pump light [28]. In this case $\mathcal{B}_+ = \mathcal{B}_-$. We here are interested in the case when one of the generated optical sidebands is decoupled from the pump light to the highest possible degree. This is possible when $\gamma_- \neq \gamma_+$.

Indeed, let us assume that $\gamma_- \gg \gamma_+$. According to Eqs. (23) and (24), in this case the detuning value Δ_+ depends on the detuning of the pump light Δ_0 much less than Δ_- . Variations of the pump frequency are nearly exactly imprinted at the Δ_- . On the other hand, both Δ_+ and Δ_- depend on the pump power. As the result the fluctuations of the generated light depend on both the frequency and power fluctuations of the pump. In this section we study the simplest case of the hyperparametric oscillator operating in the vicinity of the threshold and demonstrate that while the frequency noise of

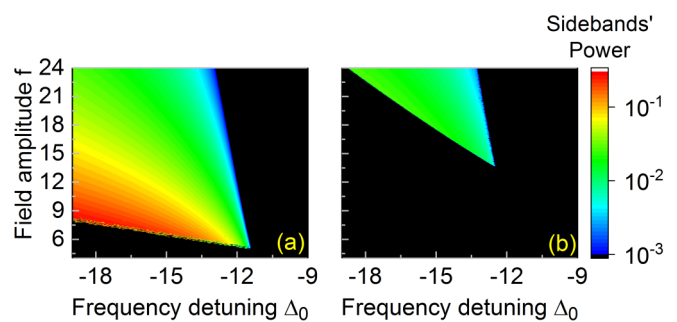


FIG. 6. Color density map plot illustrating dependence of the generated sidebands power on the detuning Δ_0 and pump amplitude f for the case of $\gamma_+ = \gamma_0$ and $\gamma_- = 10\gamma_0$ as well as $D = 15$. Panels (a) and (b) illustrate hard and soft excitation regimes, respectively. The lowest point of the plot shows the position of the oscillation threshold illustrated by Fig. 4.

the pump is indeed suppressed the fluctuations of the power become important.

A. Equations describing the fluctuations

To study phase fluctuations in the system we introduce fluctuations terms as

$$a = (|A| + \delta A)e^{i(\phi_0 + \delta\phi_0)}e^{-i\omega t}, \quad (32)$$

$$b_{\pm} = (|B_{\pm}| + \delta B_{\pm})e^{i(\phi_{\pm} + \delta\phi_{\pm})}e^{-i\tilde{\omega}_{\pm}t}, \quad (33)$$

$$F_0 = (|F| + \delta F)e^{i(\phi_{F0} + \delta\phi_{F0})}, \quad (34)$$

where the amplitude and phase fluctuation terms of the field amplitudes are related to the annihilation operators as

$$\hat{a} = \delta A + i|A|\delta\phi_0, \quad (35)$$

$$\hat{b}_{\pm} = \delta B_{\pm} + i|B_{\pm}|\delta\phi_{\pm} \quad (36)$$

and δF as well as $\delta\phi_{F0}$ stand for the classical time-dependent noise of the optical pump.

We assume that $\xi\mathcal{B}_{\pm}^2 \ll 1$ (the generated sidebands are much smaller than the pump) and write equations for the phase and amplitude fluctuations of the pump field:

$$\begin{aligned} \delta\dot{A} + \frac{|F|}{|A|} \cos\psi \delta A \\ = |F| \sin\psi (\delta\phi_0 - \delta\phi_{F0}) + \delta F \cos\psi + \text{Re}[f_0 e^{i\omega t}], \end{aligned} \quad (37)$$

$$\begin{aligned} \delta\dot{\phi}_0 + \frac{|F|}{|A|} \cos\psi (\delta\phi_0 - \delta\phi_{F0}) \\ = \left(2g|A|^2 - \frac{|F|}{|A|} \sin\psi\right) \frac{\delta A}{|A|} + \delta F \frac{\sin\psi}{|A|} + \frac{1}{|A|} \text{Im}[f_0 e^{i\omega t}]. \end{aligned} \quad (38)$$

It worth noticing that $|F| \cos\psi/|A| \sim \gamma_0$ for the unsaturated system, so the cavity modifies the noise due to the filtering function of the linear resonance. Fluctuations of the phase of the pump define the fluctuations of the pump field in the mode. Here, for the sake of shortness, we use the following notations: $\text{Re}[f_0 e^{i\omega t}] = (f_0 e^{i\omega t} + \text{adj.})/2$ and $\text{Im}[f_0 e^{i\omega t}] = (f_0 e^{i\omega t} - \text{adj.})/2i$.

A linearized set of equations for the amplitude and phase fluctuations of the sidebands are

$$\begin{aligned} \delta\dot{B}_{\pm} = \text{Re}[f_{\pm} e^{i\tilde{\omega}_{\pm}t}] \\ - g|A|^2 \sin\phi \left(\delta B_{\mp} - \frac{|B_{\mp}|}{|B_{\pm}|} \delta B_{\pm} \right) \\ - g|A|^2 \cos\phi |B_{\mp}| (2\delta\phi_0 - \delta\phi_+ - \delta\phi_-), \end{aligned} \quad (39)$$

$$\begin{aligned} \delta\dot{\phi}_{\pm} = \frac{1}{|B_{\pm}|} \text{Im}[f_{\pm} e^{i\tilde{\omega}_{\pm}t}] \\ - g|A|^2 \frac{|B_{\mp}|}{|B_{\pm}|} \sin\phi (2\delta\phi_0 - \delta\phi_+ - \delta\phi_-) \end{aligned}$$

$$\begin{aligned} + g|A|^2 \frac{|B_{\mp}|}{|B_{\pm}|} \cos\phi \left(\frac{\delta B_{\mp}}{|B_{\mp}|} - \frac{\delta B_{\pm}}{|B_{\pm}|} \right) \\ + 2g|A|\delta A \left(2 + \frac{|B_{\mp}|}{|B_{\pm}|} \cos\phi \right). \end{aligned} \quad (40)$$

We are interested in the solution of Eqs. (39) and (40) describing phase noise of the optical harmonics generated in the process. To find the solutions we have to take into account the following equations:

$$\begin{aligned} \frac{\delta\dot{B}_+}{|B_+|} - \frac{\delta\dot{B}_-}{|B_-|} \\ = g|A|^2 \sin\phi \left(\frac{|B_-|}{|B_+|} + \frac{|B_+|}{|B_-|} \right) \left(\frac{\delta B_+}{|B_+|} - \frac{\delta B_-}{|B_-|} \right) \\ - g|A|^2 \cos\phi \left(\frac{|B_-|}{|B_+|} - \frac{|B_+|}{|B_-|} \right) (2\delta\phi_0 - \delta\phi_+ - \delta\phi_-) \\ + \frac{1}{|B_+|} \text{Re}[f_+ e^{i\tilde{\omega}_+t}] - \frac{1}{|B_-|} \text{Re}[f_- e^{i\tilde{\omega}_-t}], \end{aligned}$$

$$\begin{aligned} 2\delta\dot{\phi}_0 - \delta\dot{\phi}_+ - \delta\dot{\phi}_- \\ = g|A|^2 \sin\phi \left(\frac{|B_-|}{|B_+|} + \frac{|B_+|}{|B_-|} \right) (2\delta\phi_0 - \delta\phi_+ - \delta\phi_-) \\ - 2 \left\{ g|A|^2 \left[2 + \left(\frac{|B_-|}{|B_+|} + \frac{|B_+|}{|B_-|} \right) \cos\phi \right] + \frac{|F|}{|A|} \sin\psi \right\} \frac{\delta A}{|A|} \\ + g|A|^2 \cos\phi \left(\frac{|B_-|}{|B_+|} - \frac{|B_+|}{|B_-|} \right) \left(\frac{\delta B_+}{|B_+|} - \frac{\delta B_-}{|B_-|} \right) \\ - 2 \frac{|F|}{|A|} \cos\psi (\delta\phi_0 - \delta\phi_{F0}) + 2\delta F \frac{\sin\psi}{|A|} \\ + \frac{2}{|A|} \text{Im}[f_0 e^{i\omega t}] - \frac{1}{|B_+|} \text{Im}[f_+ e^{i\tilde{\omega}_+t}] - \frac{1}{|B_-|} \text{Im}[f_- e^{i\tilde{\omega}_-t}]. \end{aligned} \quad (41)$$

Since we assumed that $\gamma_- \gg \gamma_+$, we focus on the expression for the phase noise of the light generated in the long-lived optical mode. In the vicinity of the oscillation threshold we can safely assume that $\sin\phi \simeq -1$ and $\cos\phi \simeq 0$. In this case the equation for the phase of the optical harmonic becomes

$$\begin{aligned} \delta\dot{\phi}_+ = \frac{1}{|B_+|} \text{Im}[f_+ e^{i\tilde{\omega}_+t}] \\ + g|A|^2 \sqrt{\frac{\gamma_+}{\gamma_-}} (2\delta\phi_0 - \delta\phi_+ - \delta\phi_-) + 4g|A|^2 \frac{\delta A}{|A|}. \end{aligned} \quad (42)$$

This equation should be supplied with a simplified equation for the relative phase of the pump and generated harmonics:

$$\begin{aligned} 2\delta\dot{\phi}_0 - \delta\dot{\phi}_+ - \delta\dot{\phi}_- \\ = -g|A|^2 \sqrt{\frac{\gamma_-}{\gamma_+}} (2\delta\phi_0 - \delta\phi_+ - \delta\phi_-) + 2\delta\dot{\phi}_0. \end{aligned} \quad (43)$$

We dropped the other fluctuations terms in Eq. (43) since their contributions are smaller than the impact of the similar terms in Eq. (42).

B. Solution of the equations

We have to solve Equations (37), (38), (42), and (43) to find noise of phase ϕ_+ of the light generated in the high-Q mode. To do it we utilize the Fourier transformation

$$\delta\phi_+(t) = \int_{-\infty}^{\infty} \delta\phi_+(\Omega) e^{-i\Omega t} \frac{d\Omega}{2\pi}, \quad (44)$$

and introduce single sideband phase noise in the form

$$\langle \delta\phi_+(t) \delta\phi_+(t - \tau) \rangle = \int_{-\infty}^{\infty} \mathcal{L}_+(\Omega) e^{i\Omega\tau} \frac{d\Omega}{2\pi}. \quad (45)$$

Fourier amplitudes for the fluctuational force $\text{Im}[f_+(t)]$ are introduced a similar way:

$$\text{Im}[f_+(t)] = \int_{-\infty}^{\infty} \text{Im}[f_+(\Omega)] e^{-i\Omega t} \frac{d\Omega}{2\pi}. \quad (46)$$

The simplified solution for the Fourier amplitudes can be found in the steady-state approximation, $\gamma_+ \gg \Omega$, and also under the assumption that the shot noise of the pump is much smaller than the shot noise of the generated harmonic:

$$\begin{aligned} \phi_+(\Omega) = & \frac{1}{|B_+|} \frac{\text{Im}[f_+(\Omega)]}{-i\Omega} + 2 \frac{\gamma_+}{\gamma_-} \delta\phi_{F0}(\Omega) \\ & + \frac{4g|A|^2(|F|/|A|)}{-i\Omega(|F|/|A| - 2g|A|^2 \sin\psi)} \frac{\delta F(\Omega)}{|F|}. \end{aligned} \quad (47)$$

This expression is valid since $\sin\psi$ is negative in the region of stable oscillation.

Since term f_+ represents Langevin force arising from the attenuation of light in the mode it obeys the relationships

$$\langle f_+(t) \rangle = 0, \quad (48)$$

$$\langle f_+(t) f_+^\dagger(t') \rangle = 2\gamma_+ \delta(t - t'), \quad (49)$$

$$\langle f_+^\dagger(t) f_+(t') \rangle = 0, \quad (50)$$

where $\langle \dots \rangle$ stands for ensemble averaging. Consequently,

$$\langle \text{Im}[f_+(t)] \text{Im}[f_+(t')] \rangle = \frac{1}{2} \gamma_+ \delta(t - t'), \quad (51)$$

$$\langle \text{Im}[f_+(\Omega)] \text{Im}[f_+(\Omega')] \rangle = \pi \gamma_+ \delta(\Omega + \Omega'). \quad (52)$$

$$(53)$$

The phase noise of the generated light is

$$\mathcal{L}_+(\Omega) \simeq \frac{\gamma_+}{2\Omega^2 |B_+|^2} + 4 \frac{\gamma_+^2}{\gamma_-^2} \mathcal{L}_{\phi F0}(\Omega) + \frac{\xi \gamma_0^2}{\Omega^2} RIN, \quad (54)$$

where ξ is a dimensionless parameter of the order of a unit, $\mathcal{L}_{\phi F0}(\Omega)$ is the phase noise of the pump light, and RIN is the relative intensity noise of the pump light.

Equation (54) represents the main result of the paper. It shows that the phase noise of the harmonic generated in the high-Q mode is given by the fundamental phase noise resulting from phase diffusion, where the expression connecting the expectation value of the number of photons $|B_+|^2$ and the output power P_{Bout+} is

$$|B_+|^2 = \frac{P_{Bout+}}{2\gamma_+ \hbar \omega_+}, \quad (55)$$

as well as the phase and amplitude noise of the pump light. The contribution of the phase noise of the pump is significantly suppressed, while contribution of the RIN of the pump can be significant if the noise has technical contribution $\sim \Omega^{-\zeta}$, where $\zeta > 0$. This could be standard flicker noise of the laser. However, if RIN of the pump coincides with the pump shot noise, the term becomes negligible, since we assumed that the pump has much higher power than the harmonics. Therefore, the hyperparametric oscillator allows improving the phase noise of the pump laser. The improvement is possible for an oscillation occurring at both normal and anomalous GVD, as the soft excitation regime becomes possible due to unequal decay rates of the sideband optical modes.

C. Classical transfer function

The described simplified analytical model assumes that the system has a stable dynamical attractor in the vicinity of the oscillation threshold. It is not obvious that there is a stable solution at these conditions since we are dealing with nonlinear systems where chaos, bifurcations, and other effects can occur within the parameter space that characterizes the system. Also, in the vicinity of the oscillation threshold, where fluctuations are huge, linearized analysis is no longer valid. Nonlinear effects are crucial to characterize these fluctuations. To alleviate these concerns, we perform a numerical study that clearly shows validity of the analytical model.

We have demonstrated stability islands for the oscillations in Sec. III A, in which the original set of the nonlinear differential equations (3)–(5) was solved numerically while varying parameters of the system. In this section we select the solutions for which the analytical model is valid ($\xi \mathcal{B}_\pm^2 \ll 1$) and find the transfer function of the phase fluctuations of the pump light to the phase fluctuations of the generated optical harmonics to verify if the phase modulation of the pump indeed impacts the oscillation harmonic generated in the higher Q optical mode less than the harmonic generated in the lower Q mode. Results of the simulations confirm the conclusions of the analytical calculation.

We select the realizations of the oscillations for which the pump amplitude f is as small as possible. To do it we first select the value of the GVD parameter D for the cases of identical decay rates of the sideband modes, $\gamma_\pm = \gamma_0$, as well as significantly dissimilar decay rates, $\gamma_+ = \gamma_0$ and $\gamma_- = 10\gamma_0$. The threshold conditions for these cases are shown in Figs. 1 and 3, respectively. We find that the smallest f can be used if $D = -2$ for the symmetric case and $D = -6$ for the asymmetric case.

We select next the normalized amplitude of the pumping force f to exceed the corresponding threshold only slightly and find the dependence of the power of the generated sidebands, \mathcal{B}_\pm^2 , on the frequency detuning of the pump light, Δ_0 . The initial conditions for the amplitudes of the harmonics are selected randomly within the range of 0...5. The integration time is selected to be 300 ring-down times of the cold cavity. In this way the unstable solutions decay and only stable ones are observed.

The resultant curves are shown in Fig. 7. The particular solution is stable at any Δ_0 for the symmetric decay rates. The stability is lost at the larger negative detunings for the case of

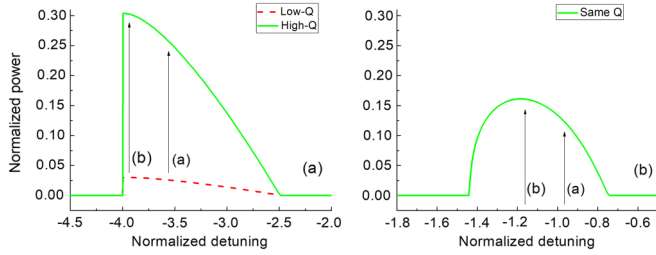


FIG. 7. Dependence of the normalized power of the generated sideband B_{\pm}^2 on the normalized frequency detuning of the pump light Δ_0 . Only stable solutions are shown. (a) The normalized pump amplitude, $f = 2.2$, for the case of $\gamma_+ = \gamma_0$ and $\gamma_- = 10\gamma_0$ as well as $D = -6$ and is a part of Fig. 5(a). (b) Pump amplitude, $f = 1.1$, for the symmetric case of $\gamma_{\pm} = \gamma_0$ as well as $D = -2$.

asymmetric decays so the left side of the curves in Fig. 7(a) is truncated. This type of instability is already taken into account in the density plot shown in Fig. 5(a).

The generated harmonics have identical normalized power in the case of symmetric decay rates. In the case of the asymmetric decays they are unequal, as predicted by Eq. (25). At the outside of the cavity, though, the actual power levels become equal, as follows from the energy conservation standpoint [Eq. (26)].

To evaluate the suppression of the phase noise of the pump light in the generated harmonics we perform simulations using the technique developed for the testing noise of Kerr frequency combs [29,32]. The external optical pumping is given by $F_0(t) = |F| \exp[i\phi_{F_0}(t)]$, where $|F|$ is the value of the amplitude of the pump light that is considered to be constant and $\phi_{F_0}(t)$ is a time-dependent phase of the pump light.

We introduce slow modulation of the pump light and find the relative power of phase modulation of the generated harmonics to infer the transfer function characterizing the impact of the phase modulation (noise) of the pump on the phase of the optical frequency harmonics. Namely, we present the normalized external force in the form

$$F_0 = |F| e^{i\kappa \cos \Omega t}, \quad (56)$$

where $\kappa \ll 1$ is a coefficient of phase modulation, and Ω is the modulation frequency (having the same meaning as the Fourier frequency we utilized in the analytical study). We assume that the modulation coefficient is much less than unity since we are interested in the study of transfer of a relatively small noise from the pump to the harmonics. We run the simulation at various Ω for the time interval exceeding the cavity ring down by factor of 300 and compare the magnitude of the phase modulation of the intracavity pump and the generated harmonics. We normalize the obtained values to the modulation magnitude of the external pump and find the power transfer efficiency as a function of the modulation frequency Ω . The results of the simulations are shown in Figs. 8 and 9.

For the case of the symmetric loading of the oscillator modes ($\gamma_{\pm} = \gamma_0$) the phase noise of the pump and harmonics is the same (Fig. 8) at small modulation frequencies ($\Omega/\gamma_0 \ll 1$). This result coincides with the prediction of the

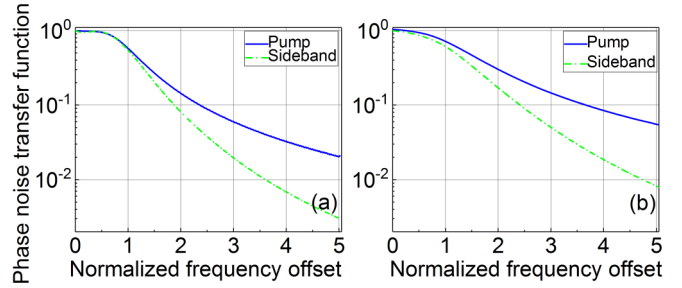


FIG. 8. Phase noise transfer function for the case of symmetric loading of the modes $\gamma_{\pm} = \gamma_0$. (a) Off-resonant and (b) resonant tuning of the pump light, as shown in Fig. 7(b). Both generated optical harmonics are characterized with the same noise transfer function with respect to the optical pump noise.

analytical model. At larger detunings the modulation (and the associated noise transfer) is suppressed due to filtering properties of the cavity. Interestingly, the filtering is stronger for the generated harmonics. It happens because the noise is filtered by both the pump and the harmonic cavity modes. In this way the noise cleaning occurs even in the symmetric loading case.

We have selected two values of the pump detuning Δ_0 to see if the saturation point in Fig. 7 makes any difference and obtained a similar result at small modulation frequencies ($\Omega/\gamma_0 \ll 1$). At larger modulation frequencies the phase modulation is filtered out faster when the oscillator operates in the unsaturated regime.

The result is drastically different for the case of the asymmetric loading of the sideband modes (Fig. 9). First, at the small modulation frequencies ($\Omega/\gamma_0 \rightarrow 0$) the modulation of the pump is suppressed by factor $4\gamma_+^2/\gamma_-^2$. This is exactly the prediction of the analytical model Eq. (54). (It worth noting that the analytical model is valid for both saturated and unsaturated regimes considered here.) Second, the numerical model shows that tuning the frequency of the pump light towards the saturation of the oscillation results in a significant reduction of the noise transfer from the pump to the harmonic generated in the high-Q mode through the entire spectral range [Fig. 9(b)]. Therefore, the system operates as a true “noise eater.”

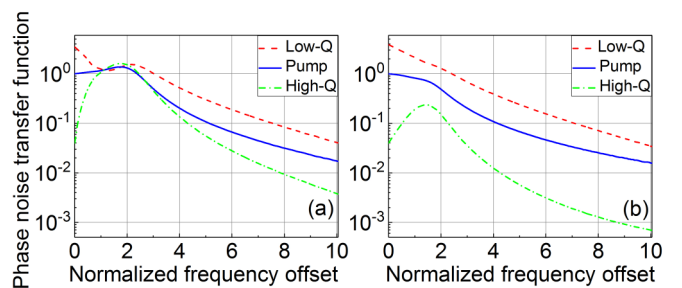


FIG. 9. Phase noise transfer function for the case of asymmetric loading of the resonator modes $\gamma_+ = \gamma_0$ and $\gamma_- = 10\gamma_0$. (a) Off-resonant and (b) resonant tuning of the pump light, as shown in Fig. 7(a). The transfer of the pump noise to the high-Q optical mode is significantly suppressed. The suppression of the phase noise of the pump light is $4\gamma_+^2/\gamma_-^2$, as predicted by Eq. (54).

Suppression of the pump phase modulation (and noise) at small frequencies results in improvement of the long-term stability of the generated light. Suppression of the pump modulation in the entire frequency range shows that indeed the spectral purity of the generated signal becomes better if compared with the pump light. In this way the numerical simulation complements the analytical study and allows us to apprehend the complete picture of the predicted phenomenon.

It is important to note that the simulation speed can be improved significantly if the frequency Ω is slowly changing in time while running the code (the pump light is considered to be chirped [29,32]). In this way we can find the modulation transfer spectrum from a single code run. The result is practically the same with respect to the method involving separate run of the code for each modulation frequency value. The chirped force method is sometimes inaccurate, though, especially at small Ω , so a careful selection of the modulation frequency range and chirp speed should be exercised. The final run is more reliable for the selection of the discrete modulation frequencies.

V. DISCUSSION

We have shown that both realizing a nonlinear optical cavity characterized with an optical spectrum having significantly dissimilar Q factors and exciting a hyperparametric oscillation in the cavity may result in an improvement of the spectral purity of the generated light. The major condition for the sizable effect is a significantly larger frequency bandwidth of one of the optical modes receiving one generated harmonic than the bandwidth of the other generated harmonic. The spectrally pure light is generated in the harmonics characterized with the higher Q factor. In this section we describe several practical ways of realizing such a cavity.

Optical modes belonging to a single-mode family of a standard monolithic optical cavity usually have nearly identical Q factors. The reason is that the optical properties of the transparent dielectrics do not change much at the scale of a few hundred GHz or smaller. The simplest way to modify the Q factors of one or several modes of the same cavity is to

introduce a narrow-band absorber to the cavity [33]. It can be an atomic or molecular absorption line or a diffraction grating selectively removing photons from the selected optical mode. Another cavity coupled to the nonlinear cavity also results in the attenuation management. Instead of an additional cavity one can use another, lower-Q, mode family belonging to the same cavity. Modes of different mode families tend to interact, and, because the mode families are characterized with different free spectral ranges, the interaction impacts not all the modes of the mode family of interest. Usage of a multidimensional quasiperiodic grating allows creating cavities with a few optical modes characterized by dissimilar bandwidth values.

Another way of engineering the Q factors is related to altering phase matching of the hyperparametric process. It was shown that creating a cavity in which the group velocity dispersion changes from a normal to an anomalous one can observe strongly nondegenerate hyperparametric scattering in which one of the harmonics is strongly shifted to the red and the other is shifted to the blue [30,34]. The frequency difference can exceed an octave, and, consequently, the Q factors of the corresponding cavity modes can be significantly different.

VI. CONCLUSION

We have analyzed the reduction of the optical phase noise in a harmonic of a resonant hyperparametric oscillator characterized by dissimilar Q factors of the optical modes involved in the oscillation process. The phenomenon occurs due to redistribution of the noise of the optical pump between the harmonics generated in the low-Q and high-Q modes of the nonlinear optical cavity. The noise reduction can be utilized for cleaning noise of semiconductor lasers integrated on photonic platforms. The method is advantageous for producing high spectral purity optical sources on a chip.

ACKNOWLEDGMENTS

The author acknowledges stimulating discussions with Prof. Irina Novikova and Prof. Eugeniy Mikhailov.

-
- [1] T. Kessler, C. Hagemann, C. Grebing, T. Legero, U. Sterr, F. Riehle, M. J. Martin, L. Chen, and J. Ye, A sub-40-mHz-linewidth laser based on a silicon single-crystal optical cavity, *Nat. Photon.* **6**, 687 (2012).
 - [2] S. N. Lea, Limits to time variation of fundamental constants from comparisons of atomic frequency standards, *Rep. Prog. Phys.* **70**, 1473 (2007).
 - [3] T. Nazarova, C. Lisdat, F. Riehle, and U. Sterr, Low-frequency-noise diode laser for atom interferometry, *J. Opt. Soc. Am. B* **25**, 1632 (2008).
 - [4] K. Predehl, G. Grosche, S. M. F. Raupach, S. Droste, O. Terra, J. Alnis, Th. Legero, T. W. Hänsch, Th. Udem, R. Holzwarth, and H. Schnatz, A 920-kilometer optical fiber link for frequency metrology at the 19th decimal place, *Science* **336**, 441 (2012).
 - [5] A. Quessada, R. P. Kovacich, I. Courtillot, A. Clairon, G. Santarelli, and P. Lemonde, The Dick effect for an optical frequency standard, *J. Opt. B* **5**, S150 (2003).
 - [6] I. Coddington, W. C. Swann, L. Lorini, J. C. Bergquist, Y. Le Coq, C. W. Oates, Q. Quraishi, K. S. Feder, J. W. Nicholson, P. S. Westbrook, S. A. Diddams, and N. R. Newbury, Coherent optical link over hundreds of metres and hundreds of terahertz with subfemtosecond timing jitter, *Nat. Photon.* **1**, 283 (2007).
 - [7] E. Ip, A. P. T. Lau, D. J. F. Barros, and J. M. Kahn, Coherent detection in optical fiber systems, *Opt. Express* **16**, 753 (2008).
 - [8] S. Webster and P. Gill, Force-insensitive optical cavity, *Opt. Lett.* **36**, 3572 (2011).
 - [9] D. R. Leibrandt, J. C. Bergquist, and T. Rosenband, Cavity-stabilized laser with acceleration sensitivity below $10^{12}g^1$, *Phys. Rev. A* **87**, 023829 (2013).

- [10] Q.-F. Chen, A. Nevsky, M. Cardace, S. Schiller, T. Legero, S. Häfner, A. Uhde, and U. Sterr, A compact, robust, and transportable ultra-stable laser with a fractional frequency instability of 10^{15} , *Rev. Sci. Instrum.* **85**, 113107 (2014).
- [11] B. Dahmani, L. Hollberg, and R. Drullinger, Frequency stabilization of semiconductor lasers by resonant optical feedback, *Opt. Lett.* **12**, 876 (1987).
- [12] L. Hollberg and M. Ohtsu, Modulatable narrow-linewidth semiconductor lasers, *Appl. Phys. Lett.* **53**, 944 (1988).
- [13] W. Liang, V. S. Ilchenko, A. A. Savchenkov, A. B. Matsko, D. Seidel, and L. Maleki, Whispering-gallery-mode-resonator-based ultranarrow linewidth external-cavity semiconductor laser, *Opt. Lett.* **35**, 2822 (2010).
- [14] P. S. Donvalkar, A. Savchenkov, and A. Matsko, Self-injection locked blue laser, *J. Opt.* **20**, 045801 (2018).
- [15] A. Savchenkov, S. Williams, and A. Matsko, On stiffness of optical self-injection locking, *Photonics* **5**, 43 (2018).
- [16] S. P. Smith, F. Zarinetchi, and S. Ezekiel, Narrow linewidth stimulated Brillouin fiber laser and applications, *Opt. Lett.* **16**, 393 (1991).
- [17] A. Debut, S. Randoux, and J. Zemmouri, Linewidth narrowing in Brillouin lasers: Theoretical analysis, *Phys. Rev. A* **62**, 023803 (2000).
- [18] A. Debut, S. Randoux, and J. Zemmouri, Experimental and theoretical study of linewidth narrowing in Brillouin fiber ring lasers, *J. Opt. Soc. Am. B* **18**, 556 (2001).
- [19] J. Geng, S. Staines, Z. Wang, J. Zong, M. Blake, and S. Jiang, Highly stable low-noise Brillouin fiber laser with ultranarrow spectral linewidth, *IEEE Photonics Technol. Lett.* **18**, 1813 (2006).
- [20] I. S. Grudinin, A. B. Matsko, and L. Maleki, Brillouin Lasing with a CaF_2 Whispering Gallery Mode Resonator, *Phys. Rev. Lett.* **102**, 043902 (2009).
- [21] K. J. Vahala, Back-action limit of linewidth in an optomechanical oscillator, *Phys. Rev. A* **78**, 023832 (2008).
- [22] S. Tallur, S. Sridaran, S. A. Bhave, and T. Carmon, Phase noise modeling of opto-mechanical oscillators, in *IEEE International Frequency Control Symposium, Newport Beach, CA* (IEEE, 2010), pp. 268–272.
- [23] A. B. Matsko, A. A. Savchenkov, and L. Maleki, Stability of resonant opto-mechanical oscillators, *Opt. Express* **20**, 16234 (2012).
- [24] K. Y. Fong, M. Poot, X. Han, and H. X. Tang, Phase noise of self-sustained optomechanical oscillators, *Phys. Rev. A* **90**, 023825 (2014).
- [25] W. Loh, J. Becker, D. C. Cole, A. Coillet, F. N. Baynes, S. B. Papp, and S. A. Diddams, A microrod-resonator Brillouin laser with 240 Hz absolute linewidth, *New J. Phys.* **18**, 045001 (2016).
- [26] M. G. Suh, Q. F. Yang, and K. J. Vahala, Phonon-Limited Linewidth of Brillouin Lasers at Cryogenic Temperatures, *Phys. Rev. Lett.* **119**, 143901 (2017).
- [27] I. S. Grudinin, H. Lee, O. Painter, and K. J. Vahala, Phonon Laser Action in a Tunable Two-Level System, *Phys. Rev. Lett.* **104**, 083901 (2010).
- [28] A. B. Matsko, A. A. Savchenkov, D. Strekalov, V. S. Ilchenko, and L. Maleki, Optical hyperparametric oscillations in a whispering-gallery-mode resonator: Threshold and phase diffusion, *Phys. Rev. A* **71**, 033804 (2005).
- [29] A. B. Matsko and L. Maleki, Noise conversion in Kerr comb RF photonic oscillators, *J. Opt. Soc. Am. B* **32**, 232 (2015).
- [30] W. Liang, A. A. Savchenkov, Z. Xie, J. F. McMillan, J. Burkhart, V. S. Ilchenko, C. W. Wong, A. B. Matsko, and L. Maleki, Miniature multioctave light source based on a monolithic microcavity, *Optica* **2**, 40 (2015).
- [31] T. Hansson, D. Modotto, and S. Wabnitz, Dynamics of the modulational instability in microresonator frequency combs, *Phys. Rev. A* **88**, 023819 (2013).
- [32] A. B. Matsko and L. Maleki, Feshbach resonances in Kerr frequency combs, *Phys. Rev. A* **91**, 013831 (2015).
- [33] Y. Jestin, A. B. Matsko, A. A. Savchenkov, and L. Maleki, Improving resonant photonics devices with sol-gel coatings, in *SPIE Laser Resonators and Beam Control XI*, edited by A. V. Kudryashov, A. H. Paxton, V. S. Ilchenko, and L. Aschke, *Proc. SPIE* **7194**, 719400 (2009).
- [34] A. B. Matsko, A. A. Savchenkov, S.-W. Huang, and L. Maleki, Clustered frequency comb, *Opt. Lett.* **41**, 5102 (2016).